



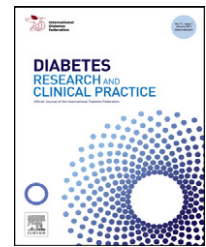
Contents lists available at ScienceDirect

Diabetes Research
and Clinical Practice

journal homepage: www.elsevier.com/locate/diabres



International
Diabetes
Federation



Adipose tissue derived mesenchymal stem cell (AD-MSc) promotes skin wound healing in diabetic rats

Mohsen Khosravi Maharlooei^a, Mansooreh Bagheri^{a,*}, Zhabiz Solhjou^a, Behnam Moein Jahromi^a, Majid Akrami^b, Lili Rohani^c, Ahmad Monabati^d, Ali Noorafshan^e, Gholamhossein Ranjbar Omrani^f

^a Cell and Molecular Medicine Research Group, Student Research Center, Shiraz University of Medical Sciences, Shiraz, Iran

^b Resident of General Surgery, Department of Surgery, Shiraz University of Medical Sciences, Shiraz, Iran

^c Laboratory for Stem Cell Research, Department of Anatomy, Shiraz University of Medical Sciences, Shiraz, Iran

^d Department of Pathology, Shiraz University of Medical Sciences, Shiraz, Iran

^e Histomorphometry & Stereology Research Centre, Shiraz University of Medical Sciences, Shiraz, Iran

^f Endocrine and Metabolism Research Centre, Department of Internal Medicine, Shiraz University of Medical Sciences, Shiraz, Iran

ARTICLE INFO

Article history:

Received 15 March 2011

Accepted 25 April 2011

Keywords:

AD-MSc

Diabetes

Wound healing

ABSTRACT

Aims: Stem cells are a new hope to ameliorate impaired diabetic wound healing. The purpose of this study was to evaluate the effect of adipose tissue derived mesenchymal stem cells (AD-MScs) on wound healing in a diabetic rat model.

Methods: Twenty-six rats became diabetic by a single intraperitoneal injection of streptozotocin. Six rats served as non-diabetic (non-DM). Diabetic rats were divided into two equal groups randomly; control and treatment. Six weeks later, a full-thickness circular excisional wound was created on the dorsum of each rat. AD-MScs were injected intra-dermally around the wounds of treatment group. PBS was applied to control and non-DM groups. The wound area was measured every other day. After wound healing completion, full thickness skin samples were taken from the wound sites for evaluation of volume density of collagen fibers, length and volume density of vessels, and numerical density of fibroblasts by stereological methods.

Results: AD-MScs accelerated wound healing rate in diabetic rats, but did not increase length and volume density of the vessels and volume density of the collagen fibers. AD-MScs decreased the numerical density of fibroblasts.

Conclusions: We concluded that AD-MScs enhances diabetic wound healing rate probably by other mechanisms rather than enhancing angiogenesis or accumulating collagen fibers.

© 2011 Elsevier Ireland Ltd. All rights reserved.

1. Introduction

Diabetes is responsible for delayed or impaired wound healing, often leading to chronic ulcer formation [1]. Chronic wounds represent a relevant clinical and socioeconomic burden [2]. The annual incidence of foot ulcers among people

with diabetes has been estimated at between 1% and 4.1%, and the annual incidence of amputation is 0.21–1.37% [3].

The mechanisms underlying impaired wound healing in diabetes are not completely understood [4]. The dynamic process of normal wound healing includes recruitment of inflammatory cells, formation of granulation tissue with

* Corresponding author. Tel.: +98 917 3201260; fax: +98 711 6243802.

E-mail addresses: mansooreh_bagheri@yahoo.com, bagherym@sums.ac.ir (M. Bagheri).

0168-8227/\$ – see front matter © 2011 Elsevier Ireland Ltd. All rights reserved.

doi:10.1016/j.diabres.2011.04.018

angiogenesis, fibroblast proliferation, and migration of keratinocytes [5]. This orderly sequence of cellular and molecular events is disrupted in diabetes, leading to compromise in wound healing [6].

Treatment of chronic wounds in diabetes has remained a challenging clinical problem [7]. Stem cell application is a new hope to treat difficult-to-heal wounds [8]. Previous studies have shown that different type of stem cells such as bone marrow-derived mesenchymal stem cells (MSCs), adult murine bone marrow (BM) stromal progenitor cells (SPCs), and adipose tissue-derived stromal cells (ATSCs)-containing atelocollagen matrix with silicon membrane are capable of enhancing wound healing rate via different mechanisms in experimental diabetic models [8–10].

In a study done by Kim et al. ATSCs accelerated wound-healing and exhibited antioxidant effects under various conditions by the activation of dermal fibroblasts and keratinocytes via the paracrine mechanism [11]. ATSCs can be obtained easily and have multi-lineage capacity, allowing them to differentiate into adipose, bone, cartilage, skeletal muscle, cardiac muscle, neuronal, hepatocytes, endothelial, hematopoietic, pancreatic, and epithelial cell types [12]. The frequency of adipose derived mesenchymal stem cells is 1:1000–1500 and is far higher than bone marrow derived stem cells [13].

Here, we studied the effect of local intra-dermal injection of adipose tissue derived mesenchymal stem cells (AD-MSCs) on wound healing rate in an experimental diabetes model. We also evaluated the AD-MSCs effect on angiogenesis, collagen accumulation, and fibroblast proliferation in the wound tissue of diabetic rats with a new stereological method.

2. Materials and methods

2.1. MSC isolation and expansion

All the procedures and materials used in this study were approved by the ethical committee of research dean in Shiraz University of Medical Sciences (SUMS). A male Sprague-Dawley rat was anesthetized with ketamine (100 mg/kg IP; Sigma-Aldrich, St. Louis, MO) and xylazine (10 mg/kg IP; Sigma-Aldrich, St. Louis, MO), and then the rat abdominal subcutaneous adipose tissue was separated under sterile condition. The tissue was chopped into small pieces. The pieces were incubated for 1 h at 37 °C in the same volume solution of 3 mg/ml collagenase type 1 from clostridium histolyticum (Sigma-Aldrich, St. Louis, MO). Thereafter, EDTA–trypsin (1× liquid, Invitrogen) was added for an additional 20 min incubation time. Afterwards, α -MEM media (1× liquid, Invitrogen, Carlsbad, CA, USA), supplemented with 10% Fetal Bovine Serum (FBS) (Gibco/Invitrogen, Carlsbad, CA, United States) was added to neutralize the trypsin. Depleted cells during centrifugation were seeded into a T25 cm² tissue culture-treated flask (Nunc, Roskilde, Denmark) and cultured in 6 ml standard growth medium at 37 °C in 5% CO₂ in a humidified incubator. Culture media consisted of α -MEM media, supplemented with 10% Fetal Bovine Serum (FBS), 1% L-glutamin (Gibco/Invitrogen, Carlsbad, CA, United States), 100 U/ml penicillin and 100 μ g/ml streptomycin (Gibco/Invitrogen, Carlsbad, CA, United States). Nonadherent cells

were removed by change of medium after 48 h. The adherent fibroblast like cells were further expanded through 6 passages [14].

2.2. MSC characterization by flowcytometry

Subcultures of passage 3 were used for flowcytometric analysis. Adherent cells were removed using a cell scraper. Then cells were washed and approximately 10⁶ cells suspended again in 100 μ l PBS for each reaction. Homogenized cell suspension was transferred into polystyrene flowcytometry tubes (BD Falcon). Cells were washed 2 times in staining buffer and fixed in 2% paraformaldehyde for 15 min at 4 °C. Again cells were washed. Non-specific antibody binding was blocked by adding 10% heat-inactivated goat serum in staining buffer for 15 min at 4 °C. Rat IgG2a Isotype Control FITC (eBioscience, San Diego, CA), rat IgG2a Isotype Control PE (eBioscience, San Diego, CA), anti rat CD11b FITC conjugated mouse antibody (Gene Tex, Inc.), anti rat CD31 FITC conjugated antibody (Serotec, Oxford, UK), anti rat CD45 FITC conjugated (Biolegend, San Diego, CA) and anti Rat CD90 PE conjugated antibody (eBioscience, San Diego, CA) were added to six different reaction tubes.

They were then incubated for 45 min at room temperature in a dark environment. Excess antibodies were washed off two times. Cells in each tube were suspended again in 0.5 ml PBS and then sorted on a FACSCalibur flowcytometer (BD Biosciences, San Jose, CA). Acquired data were then analyzed using WinMDI software [15].

2.3. Animal study

Thirty-two male Sprague-Dawley rats weighing 180–250 g were chosen for this study. Animals were kept in controlled temperature condition (25 °C) with 12 h light–dark cycles. Rats were divided into three groups randomly; treatment ($n = 13$), control ($n = 13$), and non diabetic (non-DM) groups ($n = 6$). Rats in treatment and control groups were given a single intraperitoneal injection of streptozotocin (STZ) (60 mg/kg, Sigma-Aldrich, St. Louis, MO), dissolved in sterile citrate buffer (0.05 mol/L sodium citrate, pH 4.5). The rats in non-DM group were injected intraperitoneally with equal volumes of sterile citrate buffer. Five days later, 1 cc blood was taken from each rat tail vein. After centrifuging the blood samples, plasma glucose levels were measured using a glucose analyzer (Easy Gluco Infopia Co., Ltd., Korea). Rats with plasma glucose level of higher than 280 mg/dl were considered diabetic. Six weeks later, all the rats underwent general anesthesia with ketamine (100 mg/kg IP; Sigma-Aldrich, St. Louis, MO) and xylazine (10 mg/kg IP; Sigma-Aldrich, St. Louis, MO). The dorsum was clipped free of hair. A circular full-thickness excisional wound with 1 cm diameter was created on the dorsum of each rat using a fine scissor. AD-MSCs were stained with PKH26 using red fluorescent cell linker kit (Sigma-Aldrich, St. Louis, MO) [16]. 10⁶ AD-MSCs dissolved in 1 cc phosphate buffer saline (PBS) was injected intra-dermally around the wound area of each rat in treatment group. One cc PBS was applied to the wounds of control rats in the same manner. Plasma glucose levels were measured once again one day before euthanasia.

2.4. Wound closure analysis

Photographs were taken every other day from each rat wound after debridement until wound closure. Using software composed of a point grid (designed at Histomorphometry & Stereology Research Centre, Shiraz University of Medical Sciences) wound area was calculated as follows:

$$\text{Area} = \sum P \times a/p$$

where “ $\sum P$ ” was the total points laid on the favorable area of the wound and “ a/p ” was the area associated with each point (mm^2).

$$\text{Wound closure rate (\%)} = \frac{\text{area at visit 1} - \text{area at each visit}}{\text{area at visit 1}} \times 100$$

2.5. Tissue preparation and processing

After wound closure, the rats were euthanized by ether overdose and full thickness skin biopsies ($1 \text{ cm} \times 1 \text{ cm}$) were taken from the wound site. All the samples were divided into two halves. One half of the specimens were maintained in a fresh state and underwent frozen section. The other halves were fixed in buffered formaldehyde ($\text{pH} = 7.2$), and then cut into small pieces. Nine 1 mm^2 pieces were separated from biopsies randomly. Then cylindrical paraffin blocks were prepared from these pieces. Two types of slides with different thicknesses (5 and $14 \mu\text{m}$) were made from these blocks. The cylindrical blocks were sectioned using orientator methods. Briefly, each cylindrical block was placed on a circle that was divided into 10 equal pieces using radial lines. The blocks were sectioned along the lines bearing a randomly selected number. The sectioned surface of the bar was placed on the 0-0 direction of the circle with 10 unequal cosines-weighted divisions and the second cut was done. The new surface was sectioned (5 and $14 \mu\text{m}$ thickness), and stained with Hedenhain's azan.

2.6. Fluorescent microscopy

Fresh frozen sectioned slides were studied by fluorescent microscopy with red filters to determine the presence of PKH

positive cells in epidermis, dermis and muscle layer of the wound tissue [17,18].

2.7. Volume density of the collagen fibers

Using a video microscopy system, $5 \mu\text{m}$ section slides were evaluated to measure the volume density of the collagen fibers ($V_{v(\text{collagen/dermis})}$) at magnification of 1400. A grid of 25 points was laid randomly on the live image of the microscope (Fig. 1). Fields with more than half of the points in dermis were acceptable. The number of points hitting the collagen fibers ($P_{(\text{collagen})}$) and points in dermis ($P_{(\text{dermis})}$) were counted in 10 acceptable fields for each slide. Then volume density of collagen was measured as:

$$V_{v(\text{collagen/dermis})} = \frac{P_{(\text{collagen})}}{P_{(\text{dermis})}}$$

2.8. Volume density of the vessels

The volume density of the vessels $V_{v(\text{vessel/dermis})}$ was measured as $P_{(\text{vessel})}/P_{(\text{dermis})}$ where $P_{(\text{vessel})}$ was the number of points hitting the vessels.

2.9. Length density of the vessels

$5 \mu\text{m}$ section slides were used to measure the length density (L_V) of vessels. An unbiased counting frame was laid randomly on the live image of the microscope at magnification of 1400. Any field in the dermis was acceptable. Two borders of the frame were inclusion borders and two others were exclusion ones. The number of vessels in the frame not hitting the exclusion borders (Q) was counted in different random fields for each slide [19,20]. L_V of vessels was measured as:

$$L_V = 2 \times \frac{\sum Q}{(a/f) \times \sum f}$$

where “ $\sum Q$ ” was the total number of the sectioned vessels, (a/f) was the area of the counting frame, and “ $\sum f$ ” was the total number of frames counted in each slide.

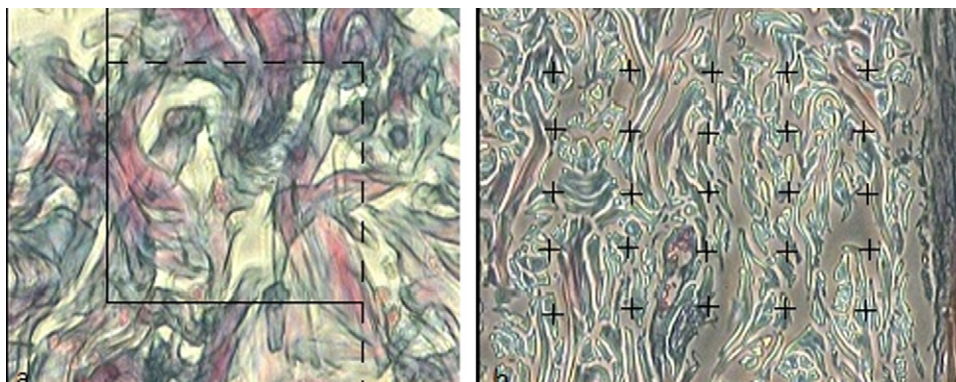


Fig. 1 – (a) An unbiased counting frame laid randomly on the live image of the microscope for calculating length density of the vessels and numerical density of the fibroblasts. (b) A grid of 25 points laid randomly on the live image of the microscope for calculating volume density of the collagen fibers and vessels.

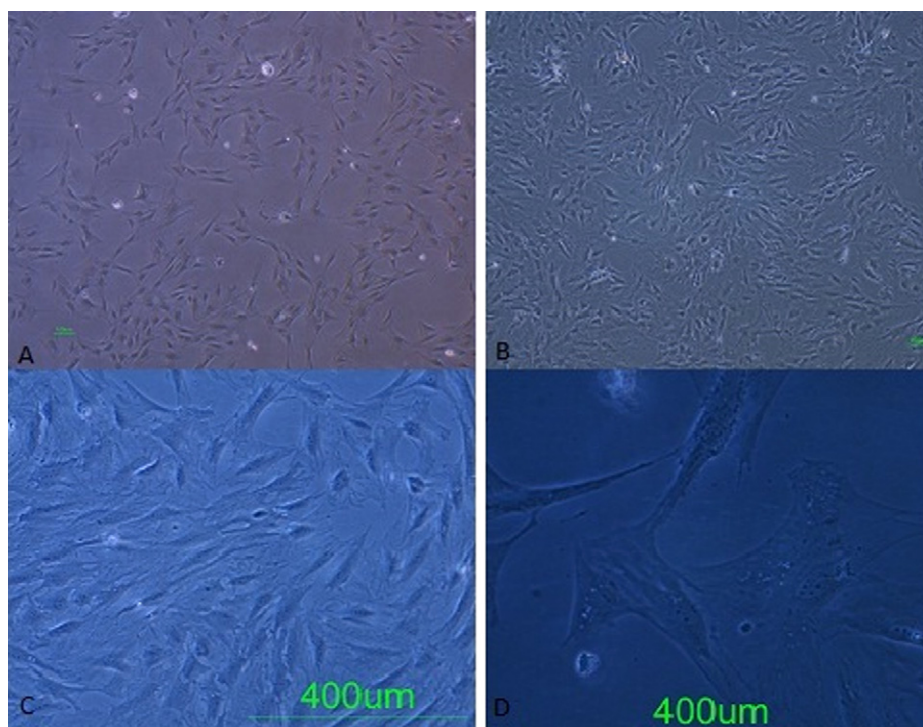


Fig. 2 – Spindle shape cultured mesenchymal stem cells at (A) passage 1, (B) passage 2, (C) passage 6, (D) passage 6 and higher magnification.

2.10. Numerical density of the fibroblasts

An unbiased counting frame was laid randomly on the live image of the microscope at magnification of 2000. 14 μm section slides were used to measure the numerical density of fibroblasts. Fibroblast nuclei located within the frame not crossing the exclusion borders and in the defined 5 μm of depth were counted in each field. For this purpose, the optical section was moved downwards in z axis traveling (depth) and a microcator (Heidenhain MT-12, Germany) showed the depth. The first 5 μm of depth was ignored and the nuclei within the second 5 μm of depth were counted [19,20]. Then numerical density (N_V) of fibroblasts was calculated as

$$N_V = \frac{\sum Q}{\sum A} \times (a/f) \times h$$

where “ $\sum Q$ ” was the number of fibroblast nuclei, “ (a/f) ” was the total area of the unbiased counting frame (1200 μm^2), “ $\sum A$ ” was total number of fields and “ h ” was the height in which the nuclei were counted (5 μm) (Fig. 1).

2.11. Statistical analysis

Values are expressed as mean \pm standard error (SE) in the text and figures. Statistical analyses were performed using SPSS software (Ver. 16). Appropriate tests (One-way ANOVA followed by Tukey post test, repeated measurement and Mann-Whitney U-test) were used to analyze the data. $P < 0.05$ was considered significant.

3. Results

All STZ-injected rats showed gross hyperglycemia and maintained it during the study. Five days after STZ injection, the mean serum glucose level was 449.4 ± 65.4 in treatment group and 429.6 ± 56.3 in control group. One day before euthanasia, the mean serum glucose level was 724.4 ± 17.6 in treatment group and 751 ± 28.3 in control group. There was no significant difference between serum glucose levels of two steps of blood sampling between the treatment and control groups.

3.1. MSC isolation and characterization

Attached cells had a high capacity of proliferation and became confluent in culture plate within three weeks. This time decreased in the following next passages. Cultured cells became spindle shape (Fig. 2). Flowcytometric analysis showed that the cells expressed CD90 and were negative for CD45, CD31, and CD11b markers.

3.2. Wound healing rate

The mean wound area was $121 \pm 29.1 \text{ mm}^2$ at the first visit. There was no significant difference in primary wound surface area among the three groups. Diabetes lowered the wound healing rate in control group compared to non-DM ($P < 0.001$). Wound closure rate was significantly increased in AD-MSCs treated rats compared to the control group ($P < 0.001$), without any significant difference with non-DM animals (Fig. 3).

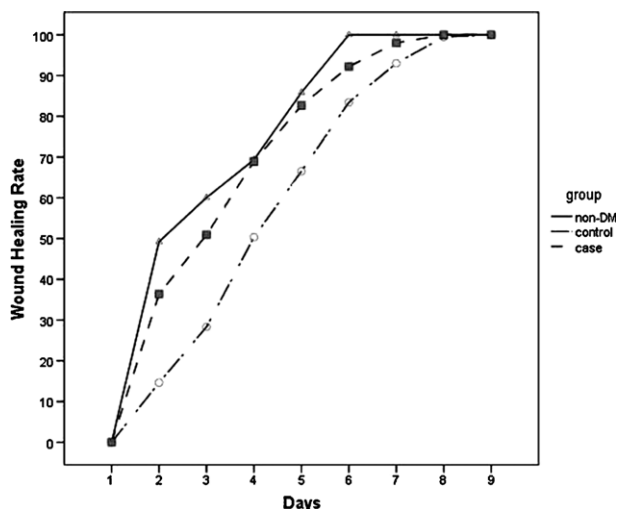


Fig. 3 – Effect of AD-MSCs on wound closure rate in diabetic rats. Wound closure rate was significantly increased in AD-MSCs-treated rats compared to control group ($P < 0.001$), without any significant difference with non-DM animals.

3.3. Fluorescent microscopy

The presence of PKH positive cells in the dermis and epidermis of the wound tissue of AD-MSCs treated rats was shown with fluorescent microscopy (Fig. 4).

3.4. Stereomicroscopic parameters

$V_{v(\text{collagen/dermis})}$ of collagen fibers, N_v of fibroblasts, L_v of vessels, and $V_{v(\text{vessel/dermis})}$ of the vessels were significantly decreased in wound tissue of control rats compared to non-DM animals ($P < 0.001$). There was no significant difference between volume density of collagen and vessel and also length density of vessels (L_v) in treatment and control groups. N_v of fibroblasts was lower in treatment group in comparison to control and non diabetic groups ($P = 0.045$) (Table 1).

4. Discussion

The present study demonstrates that AD-MSCs have the capability to increase the wound healing rate in diabetic rats. We proved the existence of AD-MSCs in both epidermis and dermis of the wound tissue with fluorescent microscopy. Contrary to our expectation, AD-MSCs did not significantly increase the volume density of the collagen fibers and the length density of the vessels evaluated by a new stereological method. AD-MSCs caused a significant reduction in numerical density of fibroblasts in the rats' wound tissue. Local intradermal injection of AD-MSCs had no effect on the plasma glucose level, so the observed effect on wound healing cannot be attributed to this parameter.

It seems that stem cell application is a new promise to treat difficult-to-heal chronic wounds such as diabetic ulcers [8]. Previous studies have shown that BM-MSCs enhance wound healing rate through increasing the angiogenesis and wound-breaking strength [6,9,21]. The suggested mechanism is that BM-mesenchymal stem cells (BM-MSCs) recruit macrophages and endothelial lineage cells into the wound by increasing vascular endothelial growth factor (VEGF)-a, insulin growth factor-1, epithelial growth factor, keratinocyte growth factor, angiopoietin-1, and stromal derived factor-1 release [22]. Application of BM-MSCs for accelerating wound healing rate has certain limitations. For example, the low frequency of progenitor cell populations and the large number of inflammatory cells in the bone marrow make it less attractive [23]. Also bone marrow aspiration is an invasive procedure.

We designed this study to evaluate AD-MSCs effect on wound healing rate in diabetes due to multiple reasons. AD-MSCs can be obtained easily and have multi-lineage capacity, allowing them to differentiate into adipose, bone, cartilage, skeletal muscle, cardiac muscle, neuronal, hepatocytes, endothelial, hematopoietic, pancreatic, and epithelial cell types [12]. The frequency of adipose derived mesenchymal stem cells is 1:1000–1500 and is far higher than bone marrow derived stem cells [13].

Previous studies have shown that adipose tissue-derived stromal cells (ATSCs) improve the wound healing rate of non-

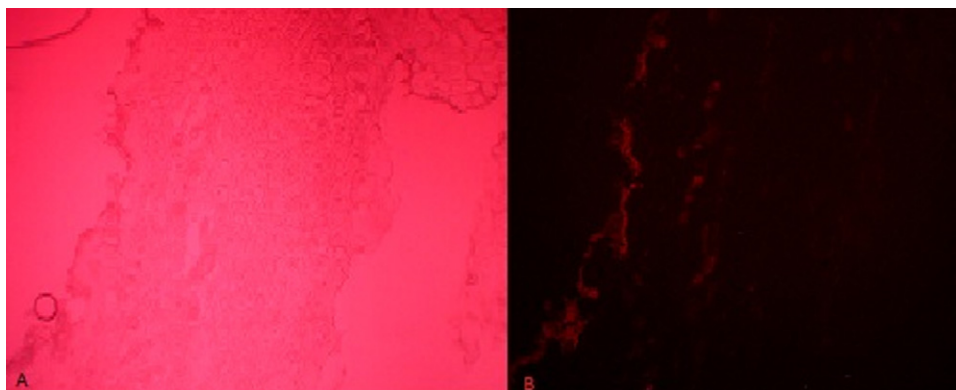


Fig. 4 – (A) Histological section of AD-MSC treated wound. (B) The same section under florescent filter showing PKH-26 positive cells (stained red). These cells are located both in epidermis and dermis.

Table 1 – Mean \pm SE of the numerical density (N_V) of the fibroblasts ($\times 10^4$ per mm^3), volume density ($V_{v(\text{collagen/dermis})}$) of the collagen fibers (%), volume density ($V_{v(\text{vessel/dermis})}$) of the vessels (%), length density (L_V) of the vessels (mm/mm^2) in non-DM, control and case groups.

Groups	N_V of fibroblasts	$V_{v(\text{collagen/dermis})}$ of collagen fibers	$V_{v(\text{vessel/dermis})}$ of the vessels	L_V of vessels
Treatment	37.9 ± 17.1	$48.5 \pm 6.3^\ddagger$	$1.54 \pm 1.09^\ddagger$	$163.6 \pm 146.2^\ddagger$
Control	54.7 ± 20.2	46.6 ± 7.4	1.39 ± 0.89	156.5 ± 118.3
Non DM	$55 \pm 16.8^\ddagger$	$42.6 \pm 4.41^\ddagger$	$1.97 \pm 1.44^\ddagger$	$195.6 \pm 169.7^\ddagger$

* $P = 0.045$ vs. treatment.
 $^\ddagger P < 0.001$ vs. control.
 $^\ddagger P$ value was not significant vs. control.

diabetic mice through increasing the angiogenesis and collagen accumulation in the wound tissue [11]. In another study, ATSCs advanced granulation tissue formation, capillary formation, and epithelialization in diabetic healing-impaired wounds [10]. Moreover, Kim et al. showed that ATSCs enhanced secretion of type I collagen by human dermal fibroblasts through regulating the mRNA levels of extracellular matrix proteins [24]. Nonetheless, our findings show that ADMSCs cannot increase the volume density of collagen fibers and the length density of the vessels, as an indicator of angiogenesis, in the wound tissue of diabetic rats. This controversy may be due to the differences between the methods to evaluate angiogenesis and collagen accumulation in the wound tissue.

Previous studies have shown the ATSCs capability to increase fibroblast in the wound tissue. Sarojini et al. showed that MSCs-conditioned medium has stimulatory effect on chemo taxis of fibroblasts [25]. Another study showed that the MSCs secretome may play a role in skin wound closure by affecting both dermal fibroblast and keratinocyte migration, along with a contribution to the formation of extracellular matrix [26]. The other controversial result of this study is that AD-MSCs injection caused a significant decrease in the number density of the fibroblast in the stem cell treated group. Our hypotheses for this observation is that the stimulatory effect of ADMSCs on the fibroblasts makes them hypertrophic, which may be the cause of decrease in numerical density of these cells in the volume unit of the wound tissue.

The result of our study showed that AD-MSCs do not have significant effect on angiogenesis and fibroblast accumulation, so other mechanisms may be involved in AD-MSCs favorable effect on diabetic wound healing. Two suggested mechanism are AD-MSCs' anti-inflammatory and anti-apoptotic effects. There is accumulating data that adult progenitor cells from adipose tissue may secrete protective factors that limit inflammation and apoptosis [27]. These progenitor cells can exert tissue protection by regulating local inflammation and repair mechanisms through secretion of protective and anti-apoptotic factors such as VEGF and hepatocyte growth factor (HGF) [28,29].

In summary, our data indicate that AD-MSCs can be promising for the treatment of difficult-to-heal diabetic wounds. AD-MSCs improved wound healing rate in diabetic rats probably through mechanisms other than enhancing angiogenesis, collagen accumulation and fibroblast proliferation. More investigations are needed to determine exact mechanism involved in this process.

Acknowledgments

This study was supported by Shiraz University of Medical Sciences (No# 4917). The authors would like to thank Dr. Hossein Baharvand for his generous donation of PKH-26. We Thank Dr. Hossein Mirkhani for his kind help in animal model experiments. We also thank Mr. Zare and Mr. Hosseini for their contribution to performing and analyzing the flowcytometric experiments.

Conflict of interest

There are no conflicts of interest.

REFERENCES

- [1] Lateef H, Abatan OI, Aslam MN, Stevens MJ, Varani J. Topical pretreatment of diabetic rats with all-trans retinoic acid improves healing of subsequently induced abrasion wounds. *Diabetes* 2005;54(3):855–61.
- [2] Barcelos LS, Duplaa C, Krankel N, Graiani G, Invernici G, Katara R, et al. Human CD133+ progenitor cells promote the healing of diabetic ischemic ulcers by paracrine stimulation of angiogenesis and activation of Wnt signaling. *Circ Res* 2009;104(9):1095–102.
- [3] Liu ZJ, Velazquez OC. Hyperoxia, endothelial progenitor cell mobilization, and diabetic wound healing. *Antioxid Redox Signal* 2008;10(11):1869–82.
- [4] Witte MB, Thornton FJ, Tantry U, Barbul A. L-Arginine supplementation enhances diabetic wound healing: involvement of the nitric oxide synthase and arginase pathways. *Metabolism* 2002;51(10):1269–73.
- [5] Medina A, Scott PG, Ghahary A, Tredget EE. Pathophysiology of chronic nonhealing wounds. *J Burn Care Rehabil* 2005;26(4):306–19.
- [6] Kwon DS, Gao X, Liu YB, Dulchavsky DS, Danyluk AL, Bansal M, et al. Treatment with bone marrow-derived stromal cells accelerates wound healing in diabetic rats. *Int Wound J* 2008;5(3):453–63.
- [7] Jeffcoate WJ, Harding KG. Diabetic foot ulcers. *Lancet* 2003;361(9368):1545–51.
- [8] Falanga V, Iwamoto S, Chartier M, Yufit T, Butmarc J, Kouttab N, et al. Autologous bone marrow-derived cultured mesenchymal stem cells delivered in a fibrin spray accelerate healing in murine and human cutaneous wounds. *Tissue Eng* 2007;13(6):1299–312.
- [9] Javazon EH, Keswani SG, Badillo AT, Crombleholme TM, Zoltick PW, Radu AP, et al. Enhanced epithelial gap closure

- and increased angiogenesis in wounds of diabetic mice treated with adult murine bone marrow stromal progenitor cells. *Wound Repair Regen* 2007;15(3):350–9.
- [10] Nambu M, Kishimoto S, Nakamura S, Mizuno H, Yanagibayashi S, Yamamoto N, et al. Accelerated wound healing in healing-impaired db/db mice by autologous adipose tissue-derived stromal cells combined with atelocollagen matrix. *Ann Plast Surg* 2009;62(3):317–21.
- [11] Kim WS, Park BS, Sung JH. The wound-healing and antioxidant effects of adipose-derived stem cells. *Expert Opin Biol Ther* 2009;9(7):879–87.
- [12] Zuk P, Mizuno H, Mizuno H, Huang J, Furtrell JW, Katz AJ, et al. Multilineage cells from human adipose tissue: implications for cell-based therapies. *Tissue Eng* 2001;7:211–28.
- [13] De Ugarte DA, Morizono K, Elbarbary A, Alfonso Z, Zuk PA, Zhu M, et al. Comparison of multi-lineage cells from human adipose tissue and bone marrow. *Cells Tissues Organs* 2003;174(3):101–9.
- [14] Pittenger MF, Mackay AM, Beck SC, Jaiswal RK, Douglas R, Mosca JD, et al. Multilineage potential of adult human mesenchymal stem cells. *Science* 1999;284(5411):143–7.
- [15] Rohani L, Karbalaie K, Vahdati A, Hatami M, Nasr-Esfahani MH, Baharvand H. Embryonic stem cell sphere: a controlled method for production of mouse embryonic stem cell aggregates for differentiation. *Int J Artif Organs* 2008;31(3):258–65.
- [16] Messina LM, Podrazik RM, Whitehill TA, Ekhterae D, Brothers TE, Wilson JM, et al. Adhesion and incorporation of lacZ-transduced endothelial cells into the intact capillary wall in the rat. *Proc Natl Acad Sci U S A* 1992;89(24):12018–22.
- [17] Nagaya N, Kangawa K, Itoh T, Iwase T, Murakami S, Miyahara Y, et al. Transplantation of mesenchymal stem cells improves cardiac function in a rat model of dilated cardiomyopathy. *Circulation* 2005;112(8):1128–35.
- [18] Kunter U, Rong S, Djuric Z, Boor P, Muller-Newen G, Yu D, et al. Transplanted mesenchymal stem cells accelerate glomerular healing in experimental glomerulonephritis. *J Am Soc Nephrol* 2006;17(8):2202–12.
- [19] Muhlfield C, Nyengaard JR, Mayhew TM. A review of state-of-the-art stereology for better quantitative 3D morphology in cardiac research. *Cardiovasc Pathol* 2010;19(2):65–82.
- [20] Garcia Y, Breen A, Burugapalli K, Dockery P, Pandit A. Stereological methods to assess tissue response for tissue-engineered scaffolds. *Biomaterials* 2007;28(2):175–86.
- [21] Estrada R, Li N, Sarojini H, An J, Lee MJ, Wang E. Secretome from mesenchymal stem cells induces angiogenesis via Cyr61. *J Cell Physiol* 2009;219(3):563–71.
- [22] Chen L, Tredget EE, Wu PY, Wu Y. Paracrine factors of mesenchymal stem cells recruit macrophages and endothelial lineage cells and enhance wound healing. *PLoS One* 2008;3(4):e1886.
- [23] Herdrich BJ, Lind RC, Liechty KW. Multipotent adult progenitor cells: their role in wound healing and the treatment of dermal wounds. *Cytotherapy* 2008;10(6):543–50.
- [24] Kim WS, Park BS, Sung JH, Yang JM, Park SB, Kwak SJ, et al. Wound healing effect of adipose-derived stem cells: a critical role of secretory factors on human dermal fibroblasts. *J Dermatol Sci* 2007;48(1):15–24.
- [25] Sarojini H, Estrada R, Lu H, Dekova S, Lee MJ, Gray RD, et al. PEDF from mouse mesenchymal stem cell secretome attracts fibroblasts. *J Cell Biochem* 2008;104(5):1793–802.
- [26] Walter MN, Wright KT, Fuller HR, MacNeil S, Johnson WE. Mesenchymal stem cell-conditioned medium accelerates skin wound healing: an in vitro study of fibroblast and keratinocyte scratch assays. *Exp Cell Res* 2010;316(7):1271–81.
- [27] Wang M, Crisostomo PR, Herring C, Meldrum KK, Meldrum DR. Human progenitor cells from bone marrow or adipose tissue produce VEGF, HGF, and IGF-I in response to TNF by a p38 MAPK-dependent mechanism. *Am J Physiol Regul Integr Comp Physiol* 2006;291(4):880–4.
- [28] Wang Y, Ahmad N, Wani MA, Ashraf M. Hepatocyte growth factor prevents ventricular remodeling and dysfunction in mice via Akt pathway and angiogenesis. *J Mol Cell Cardiol* 2004;37(5):1041–52.
- [29] Wang Y, Haider HK, Ahmad N, Xu M, Ge R, Ashraf M. Combining pharmacological mobilization with intramyocardial delivery of bone marrow cells over-expressing VEGF is more effective for cardiac repair. *J Mol Cell Cardiol* 2006;40(5):736–45.